Iranian Journal of Hydrogen & Fuel Cell 1(2015) 35-46

Iranian Journal of Hydrogen & Fuel Cell

IJHFC

Journal homepage://ijhfc.irost.ir

Modeling heat and mass transfer in laminar forced flow between parallel plates with suction or injection boundary conditions

Hassan Hassanzadeh[1,*], Mozafar Ali Mehrabian[2]

[1]Department of Mechanical Engineering, University of Birjand, Birjand, Iran
[2] Department of Mechanical Engineering, Shahid Bahonar University of Kerman, Kerman, Iran

Article Information

Article History:

Received:
27 September 2015
Received in revised form:
18 October 2015
Accepted:
20 October 2015

Keywords

Modeling
Developing flow
Heat and Mass transfer
Channel.

Abstract

A numerical model was developed to simulate the transport phenomena of a flow between two parallel plates with one porous and one non-porous (or impermeable) wall. The continuity and momentum equations were solved first, assuming the suction or injection is uniform and wall Reynolds number is in the range of $-5 \le \mathrm{Re}_w \le +5$. The results show that at a constant inlet and wall Reynolds number, the friction factor on the porous wall with suction was bigger than that with injection, but the axial non-dimensional pressure drop with injection was larger than the pressure drop in the fully developed flow between impermeable plates and also larger than the pressure drop with suction. This is because of the net increase of the mean velocity of flow along the channel when injection is imposed. In the presence of suction the pressure drop is controlled by the suction rate and approaches a constant value as the inertia and viscous forces are counterbalanced in the flow. The energy equationwas solved independently assuming a constant suction or injection rate of air in the porous wall using different thermal boundary conditions. The results show that the Nusselt number distribution along the channel depends on the thermal boundary conditions imposed on porous and non-porous walls. The thermal characteristics also depend on whether suction or injection occurs through the porous wall.

1. Introduction

Due to its application in nuclear reactors, gas turbine combustion chambers, solar collectors and electrochemical systems such as fuel cells, the fluid flow and heat transfer in channels with mass transfer at the boundary has received a great deal of attention in the past. Two major approaches exist for the analysis of the channel flow. The first approach is based on a theoretical approximation to investigate the variation of flow structure [1, 2]. The second approach uses computational fluid dynamics (CFD) techniques to examine the two or three-dimensional flow in the channels [3-12]. Both approaches are based on earlier work done on laminar channel flow with injection or suction boundary conditions.

*Corresponding Author's E-mail address: h.hassanzadeh@birjand.ac.ir

Berman [1] presented the first complete analysis of flow between two porous walls. He derived the proper form of the equations of motion and stream function for viscous, incompressible flow and uniform suction or injection. He solved the governing equations by the perturbation method. White et al. [2] obtained a series solution for this problem that was valid at all Reynolds numbers. They also obtained limiting solutions for high and low Reynolds numbers with both suction and injection. The hydrodynamic entry length in laminar flow between parallel porous plates for constant and variable fluid properties, uniform suction and injection, with uniform and parabolic entry velocity profiles have been investigated by Doughty and Perkins [3]. They solved the continuity and axial momentum equations by finite-difference analysis and gave two correlations for the length required for converting the developing flow into the developed flow when injection or suction is imposed. The results show that when the wall Reynolds number is equal to the entry Reynolds number the converting length for flow with suction is smaller than that with injection. The results also indicate that when increasing the wall Reynolds number the entry length in flow with suction is decreased, while it is increased in flow with injection. Doughty and Perkins [4] simulated the thermal entry problem for laminar flow between parallel porous plates considering constant fluid properties and constant and equal wall temperatures. Doughty and Perkins [5] also simulated the thermal and combined entry problem in laminar flow between parallel porous plates considering constant fluid properties for uniform suction and injection at constant and equal heat fluxes. They revealed that the Nusselt number for porous plates in the case of constant heat flux is higher than that for the case of constant wall temperature. This comparison is made when the Peclet number is the same for the porous walls. A similar conclusion is made for these two boundary conditions when the walls are non-porous. The effect of injection is to increase the thermal entry length continuously and monotonically, in both cases. Raithby and Knudsen [6] simulated the hydrodynamic developing laminar flow at constant fluid properties in a duct with suction and blowing. Rhee and Edwards [7] simulated the thermal and hydrodynamic laminar flow in a flat plate duct composed of one porous and one non-porous wall. In their study the channel end was closed off, uniform suction was imposed on one wall and uniform temperature or heat flux was prescribed independently at each wall. Numerical results were obtained for Pr = 0.7 and $0.5<Re_w<10$. The hydrodynamics and mass transfer of a channel made of one porous wall and one non-porous wall with the channel end closed off has also been studied by Lessner and Newman [8].

The friction and heat transfer characteristics of fully developed laminar flow in a porous tube with constant wall temperature were simulated by Kinney [9] when the wall Reynolds number was in the range of $-20<Re_w<5$. The effect of mass injection to increase the wall heat transfer was verified. Hwang and Cheng [10] simulated the flow in a square duct when one porous wall was subject to a constant heat flux, while the other three walls were adiabatic and impermeable and the wall Reynolds number was in the range of $-20 < Re_w<20$. Yuan et al. [11] simulated the fully developed laminar flow in rectangular ducts with combined thermal boundary conditions, constant heat flux at one wall and constant temperature at the other walls. It was revealed that the Nusselt number is sensitive to the boundary conditions. They also investigated the fully developed laminar flow in ducts of rectangular and trapezoidal cross-sections with one porous wall subject to mass transfer and combined thermal boundary conditions [12]. It was revealed that mass injection through one wall increases the friction factor and decreases the Nusselt number.

Hassanzadeh et al. [13] simulated the developing laminar flow in proton exchange membrane fuel cell channels with suction of oxygen and hydrogen in the cathode and anode channels, respectively. Thermal boundary conditions on porous and non–porous walls were uniform heat flux and uniform temperature, respectively.

In the majority of the above literature the energy equation was solved using one and only one thermal boundary condition. This condition was either uniform

temperature on both walls, uniform heat flux on both walls, or uniform temperature on one wall and uniform heat flux on the other wall. The present paper is probably unique from the aspect that the energy equation was solved using all possible boundary conditions. The flow and mass transfer analyses were also presented in developing flow between two parallel plates, one porous and the other one impermeable.

2. Analysis

A two-dimensional, horizontal parallel plate channel is shown schematically in Figure 1. The upper wall of the channel is porous while the lower wall is non-porous. Air, with constant thermodynamic properties, flows steadily in the channel. The flow is laminar external forces, compression work and viscous dissipation are neglected. The injection or suction occurs through the porous wall uniformly and are described by the wall Reynolds number,

$$\mathrm{Re}_w = \frac{v_w D_h}{\vartheta} \tag{1}$$

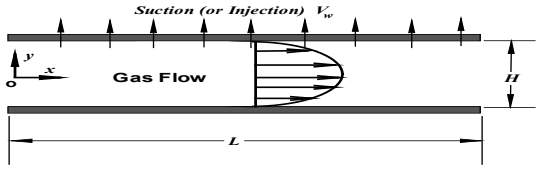

Fig. 1. Schematic diagram of flow channel and coordinate system.

where v_w is the mass transfer velocity, D_h is the hydraulic diameter which is twice the plate spacing and ϑ is the kinematic viscosity. In this study, Re_w is positive for injection and negative for suction. The injected or sucked fluid has the same temperature as the porous wall.

2.1. Governing Equations

The governing equations are the conservation of mass, momentum and energy for an incompressible Newtonian fluid at steady state conditions and are written as follows:

$$\nabla.(\rho\vec{V}) = 0 \tag{2}$$

$$\vec{V}.\nabla(\rho V) = -\nabla P + \mu\nabla^2 V \tag{3}$$

$$\vec{V}.\nabla(\rho c_p T) = k\nabla^2 T \tag{4}$$

In these relations, T is the temperature, ρ the density, μ the viscosity, c_p the specific heat at constant pressure, and k the thermal conductivity.

2.2. Boundary Conditions

The boundary conditions are:
At the inlet, x = 0:

$u=u_0$ and $T=T_0$.

At the non-porous wall, $y=-H/2$:

$u=0$, $v=0$ and $T=T_w$ (or q=const.)

At the porous wall, $y=H/2$:

$u=0$, $v=-v_w$ for suction ($v=-v_w$ for injection), q=const. (or T=const.)

At the outlet, $x=L$:

The channel is assumed sufficiently long so that the velocity and temperature fields are fully developed; therefore, the flow parameters are independent of x.

2.3. Additional Equations

The friction coefficient (C_f) and Nusselt number (Nu) are the important parameters to be calculated in the flow channel. The friction factor is related to the flow rate and the Nusselt number is related to heat transfer in the flow channel.

The fanning friction coefficient C_f is defined as the ratio of the wall shear stress $\tau_w = \mu\partial u / \partial y\big|_w$ to the flow kinetic energy per unit volume [14]:

$$C_f = \frac{\tau_w}{\frac{1}{2}\rho u_m^{\,2}} \tag{5}$$

Where, u_m is the mean flow velocity and is defined as:

$$u_m = \frac{\int u dA}{A} \tag{6}$$

When mass transfer occurs, the value of u_m is not constant along the channel and its value can be derived from mass balance in the duct. Assuming that the suction or injection flow rate is constant, the mean value of velocity changes linearly along the channel, and can be written as:

$$u_m(H) = u_0(H) + v_w x$$

Where, v_w is positive for injection and negative for suction. Rearranging for u_m we obtain:

$$u_m = u_0\left(1 + \frac{x}{H}\frac{\mathrm{Re}_w}{\mathrm{Re}_0}\right) \tag{7}$$

Where

$$\mathrm{Re}_0 = \frac{u_0 D_h}{\vartheta} \quad \text{and} \quad \mathrm{Re}_w = \frac{v_w D_h}{\vartheta} \tag{8}$$

For a given geometry, local C_f for laminar flow is independent of the surface roughness and depends on the flow condition as represented by and wall Reynolds number as:

$$C_f = f_1(\mathrm{Re}, \mathrm{Re}_w, x/D_h) \tag{9}$$

The Nusselt number as a dimensionless representation of the convective heat transfer is commonly defined as [15]:

$$Nu \equiv \frac{h_H D_h}{k} \tag{10}$$

where h_H is the convection heat transfer coefficient, which in the absence of suction or injection is defined as:

$$h_H = \frac{-k\,\partial T/\partial y\big|_{wall}}{T_w - T_m} = \frac{q_w}{T_w - T_m} \tag{11}$$

Where, T_w is the surface temperature. T_w is constant at a constant temperature boundary condition and is not constant at a heat flux constant boundary condition, and T_m is the mean temperature of the flow in the cross-section and is defined as [16]:

$$T_m = \frac{\int TudA}{\int udA} \tag{12}$$

For a given geometry, local *Nu* depends on the flow condition as represented by Re and relative effectiveness of momentum and heat transfer by diffusion in the velocity and thermal boundary layers, Pr and suction wall Reynolds number, Re_w. Therefore, the Nusselt number should have the functional form:

$$Nu = f_2(\mathrm{Re}, \mathrm{Pr}, \mathrm{Re}_w, x/D_h) \tag{13}$$

When the mass transfer occurs due to suction or injection through a porous wall, the total Nusselt number for the channel can be derived from an energy balance for a fluid element in the channel. Because $\mathrm{Re}_0 >> \mathrm{Re}_w$, the mass flow at the porous wall is much smaller than the main stream flow, therefore $(du_m/dx \approx 0)$ and the total heat transfer rate is:

$$q_t = -\rho c_P u_m H \frac{dT_m}{dx} + \rho c_P v_w (T_w - T_m) \tag{14}$$

Dividing this equation by $(T_w - T_m)D_h/k$ and rearranging we have,

$$Nu_t = \frac{q_t}{T_w - T_m}\frac{D_h}{k} = \mathrm{Re}_m\,\mathrm{Pr}\,H\frac{d\theta}{dx} + \mathrm{Re}_w\,\mathrm{Pr} \tag{15}$$

Where

$$\theta = (T_m - T_0)/(T_m - T_w) \quad \text{and} \quad \mathrm{Re}_m = u_m D_h/\vartheta$$

The first term on the right-hand side in Eq. 17 is the Nusselt number without mass transfer, , and the second term is the Nusselt number due to mass transfer, . Therefore, the total Nusselt number can be written as:

$$Nu_t = Nu_f + Nu_m \tag{16}$$

Note that Nu_m is negative for suction and positive for injection.

3. The solution method and code validation

The conservation equations (Eqs. 2-4) were discretized using the finite volume method [17]. The pressure–velocity coupling was treated by the SIMPLE algorithm with the incompressible form of the pressure correction equation. The convection diffusion terms were treated by the power law scheme. A staggered grid system was introduced in order to eliminate the numerical checker board oscillations encountered with the single grid system. In this arrangement, temperature and pressure equations are discretized and computed on the main grid, whereas the velocities are computed at the staggered nodes located mid-way between the main grid nodes. The set of algebraic equations was solved using the TDMA algorithm [18]. A grid refinement study was carried out, and it was found that a 30x120 non-uniform and symmetrical grid in x and y directions with an expansion factor of 1.05 was sufficient to provide grid-independent results.

In order to validate the accuracy of the solution it was applied to a duct with different thermal boundary conditions. The simulation results are compared with the previous results available in the literature as shown in Figure 2.

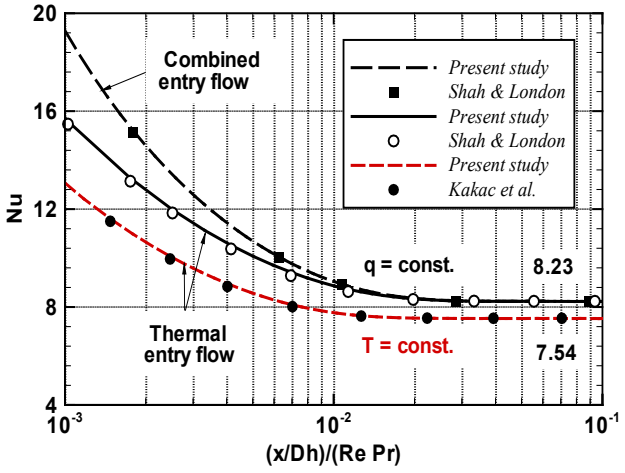

Fig. 2. Comparison of the present results with Shah and London [14], and Kakac et al. [19].

In Figure 2, the present numerical results for the Nusselt number with constant heat flux, where both velocity and temperature at the inlet are uniform, are compared with the results obtained by Shah and London [14]. The results for the Nusselt number with constant heat flux for the thermal entry flow, where the temperature at the inlet is uniform, are again compared with predictions of Shah and London [14]. The results for the Nusselt number with constant temperature for the thermal entry flow, where temperature at the inlet is uniform, are also compared with predictions of Kakac et al. [19]. The data of this reference were obtained using an empirical equation having ±3% deviation from theoretical results for the thermal entry problem in parallel plate channels with constant temperature on both walls. The present results are in good agreement with those results.

The present numerical results for the Nusselt number for the constant surface heat flux are compared with the results of Doughty and Perkins [4] in Figure 3. Both sets of results are obtained for a thermal entry problem in a channel with parallel porous walls and suction or injection on both walls. Again, the present numerical results are in good agreement with those of Doughty and Perkins [4]. These comparisons confirm that the present numerical method and the computer code are adequate in simulating the flow situations in the PEM fuel cell flow.

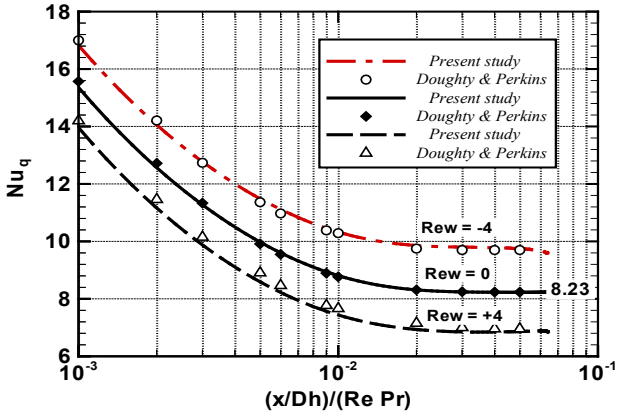

Fig. 3. Comparison of the present results with predictions of Doughty and Perkins [3] for parallel porous walls at constant heat flux on both walls.

4. Results and Discussion

The flow and heat transfer are analyzed in a horizontal parallel plate channel composed of a porous and a non-porous wall. Assuming the fluid properties are constant, the continuity and momentum equations are independent of the energy equation; therefore, the results are obtained in two parts:

Flow analysis

In this part, the air flow with suction or injection of air in the porous wall is simulated. To understand the behaviour of air flow in the channel, parameters such as velocity, pressure loss and shear stress in the channel at different wall Reynolds numbers and locations are obtained.

Heat transfer analysis

In this part, the results of solving the energy equation are presented. The Nusselt number in the channel at different locations and wall Reynolds numbers with different boundary conditions are obtained.

4.1. Flow in the channel with porous and non-porous walls imposed to suction or injection.

As mentioned before, the fluid properties are constant; therefore the continuity and momentum equations are independent of the energy equation. The flow parameters are presented in Figures 4, 5, 6, and 7. In Figure 4 the development of the x-component of velocity at different locations along the channel (x direction) is presented for the wall Reynolds number of Re_w=-8. It is seen that the velocity decreases due to the suction at the porous wall and the velocity peak shifts towards the porous wall, therefore the velocity gradient and consequently the shear stress increased on the porous wall and decreased on the non-porous wall along the flow direction. The corresponding streamlines clearly show the fluid particle motion and the suction of channel flow into the porous wall.

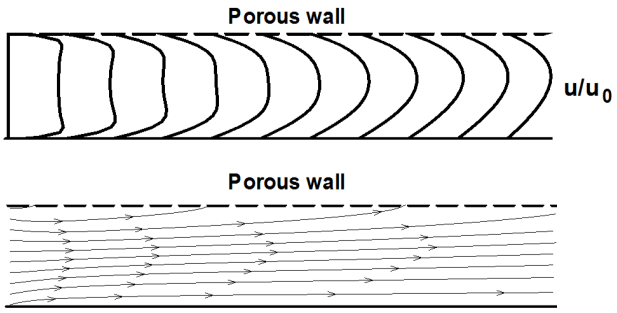

Fig. 4. The velocity distribution and streamlines along the channel at Re_0=200.

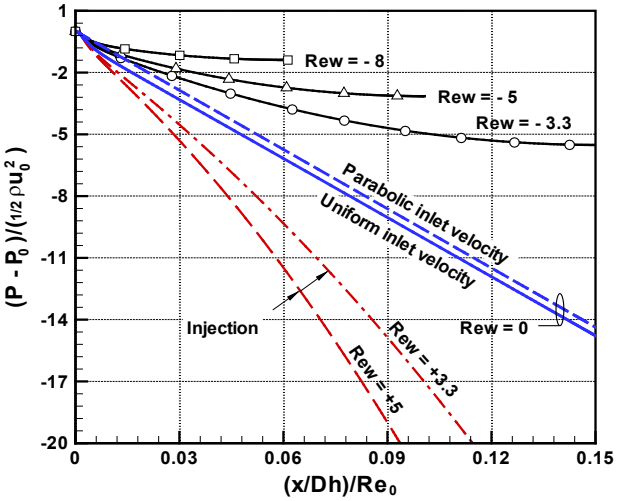

Fig. 5. Distribution of non-dimensional pressure drop along the channel at different wall Reynolds numbers at Re_0=175.

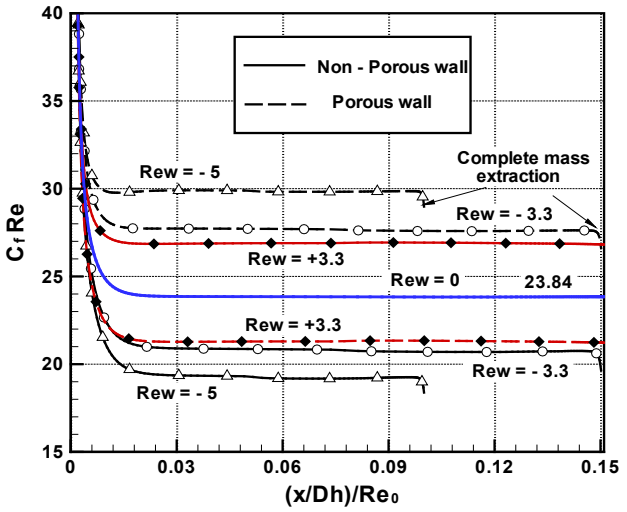

Fig. 6. Distribution of skin friction on both walls at different wall Reynolds numbers at Re_0=175.

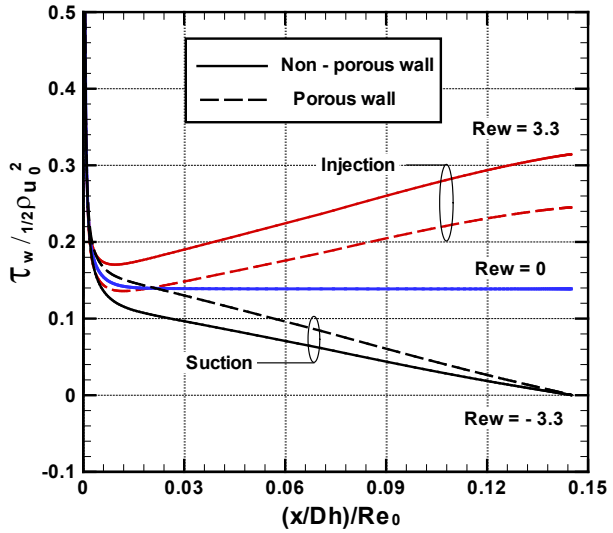

Fig. 7. Distribution of non dimensional shear stress on both walls at different wall Reynolds numbers at Re_0=175.

Figure 5 shows the non-dimensional pressure drop along the flow channel in the presence and/or absence of suction and injection at the porous wall. It is seen that without suction and injection (impermeable wall), or for the wall Reynolds number of Re_w=0, the pressure loss for uniform velocity distribution at the channel inlet is always larger than the corresponding case of the parabolic velocity profile at the channel inlet (equivalent to a fully developed flow) for the same Reynolds number. However, when the flow developed in the former case, the pressure gradients in both cases became identical, as expected, and the two lines become parallel as seen in Figure 4. When fluid is injected at the porous wall, the pressure loss becomes larger than the corresponding values for the impermeable flow (Re_w=0), because the mean flow velocity increased along the channel. Additional pressure drop is necessary to overcome the flow resistance induced by the injected fluid flow. With the suction boundary condition at the porous wall, pressure loss becomes smaller since the velocity in the channel is reduced. At low suction rates, the pressure decrease along the channel is mostly due to the viscous forces. However, at higher suction rates pressure tends to approach to a constant value as the inertia and viscous forces are counterbalanced.

Distribution of skin friction (i.e. C_fRe) in the main flow direction on the porous and non-porous walls is shown in Figure 6. The local values of the friction coefficient (C_f) and local Reynolds number (Re) are calculated based on the local mean velocity in the channel. The mean velocity in the presence of suction or injection at the porous wall is variable along the channel. It is seen that in the vicinity of the channel inlet, the values of C_f friction coefficient for all three cases become constant and the value of for the fully developed impermeable flow (Re_w=0) becomes equal to 23.84, as expected from the analytical solution. It is also interesting to notice that when suction occurs, the friction coefficient in the porous wall is always larger than the corresponding value for the nonporous wall at any location in the channel. However, it is exactly the opposite for the case of fluid injection at the porous wall. This is due to the suction boundary conditionwhere the boundary layer near the porous wall is decreased, whereas it is increased for the injection boundary condition.

The dimensionless shear stress distribution along the channel is drawn in Figure 7 for the inlet Reynolds number of Re_0=200. The results are shown for three different cases, namely when suction occurs (Re_w =-3.3), when there is no suction or injection (Re_w =0), and when injection occurs (Re_w =+3.3). The figure shows that in the entrance region the shear stress has its maximum value for the three cases mentioned above. As flow proceeds along the channel the walls are exposed to the highest shear stress when suction occurs and to the lowest shear stress when injection occurs. It is also noticed that when suction occurs the shear stress on the porous wall is more than that on the impervious wall, and the shear stress on both walls is reduces gradually and approaches zero at the end of channel. This is because of decreasing the mean flow velocity and discharging the fluid. When injection occurs, the shear stress behavior is opposite; it increases along the channel because of increasing mean flow velocity. In the entrance region, however, the shear stress on the porous wall is greater than that on the impervious wall. This trend is reversed when the flow totally enters the channel.

4.2. Constant heat flux on porous wall and constant temperature on non-porous wall

Figure 8(A) shows the variation of the local Nusselt number on both walls at different wall Reynolds numbers for constant heat flux at the porous wall and constant temperature at the non-porous wall. It is seen that the Nusselt number at the porous wall has the largest value for suction (Re_w<0), second for Re_w=0 and the smallest value for injection boundary condition (Re_w>0). This is because when suction occurs, the value of T_w-T_m is reduced due to fluid extraction and consequently the Nusselt number is increased. The opposite is true for the injection case. The Nusselt number at the non-porous wall is equal to zero near the inlet of the channel, since the temperature on the non-porous wall is assumed to be equal to the inlet temperature, T_0. As a result, heat transfer to the non-porous wall occurs only when the fluid in the channel is heated by the heat released from the porous wall. As shown in the figure, heat transfer to the non-porous wall roughly starts at the non-dimensional location of $(x/D_k)/(Re_0\ Pr)$=0.01. For non-dimensional axial values less than 0.1, the Nusselt number at the non-porous wall is nearly independent of the wall Reynolds number for the cases investigated in Figure 8.

Figure 8(B) shows the distribution of total Nusselt numbers along the channel. It is seen that beyond the entrance region near the channel inlet, the values of the total Nusselt number for different values of Rew become constant. Although the Nusselt number on the porous and non-porous wall is not constant along the channel, the total value (average value) for the channel approaches a constant value. The total Nusselt number for suction is more than that for injection and increases as the wall Reynolds number increases.

4.3. Constant heat flux on non-porous wall and constant temperature on porous wall

Figure 9(A) shows the variation of the local Nusselt number on both walls at different wall Reynolds numbers for constant heat flux at the non-porous wall and constant temperature at the porous wall. The

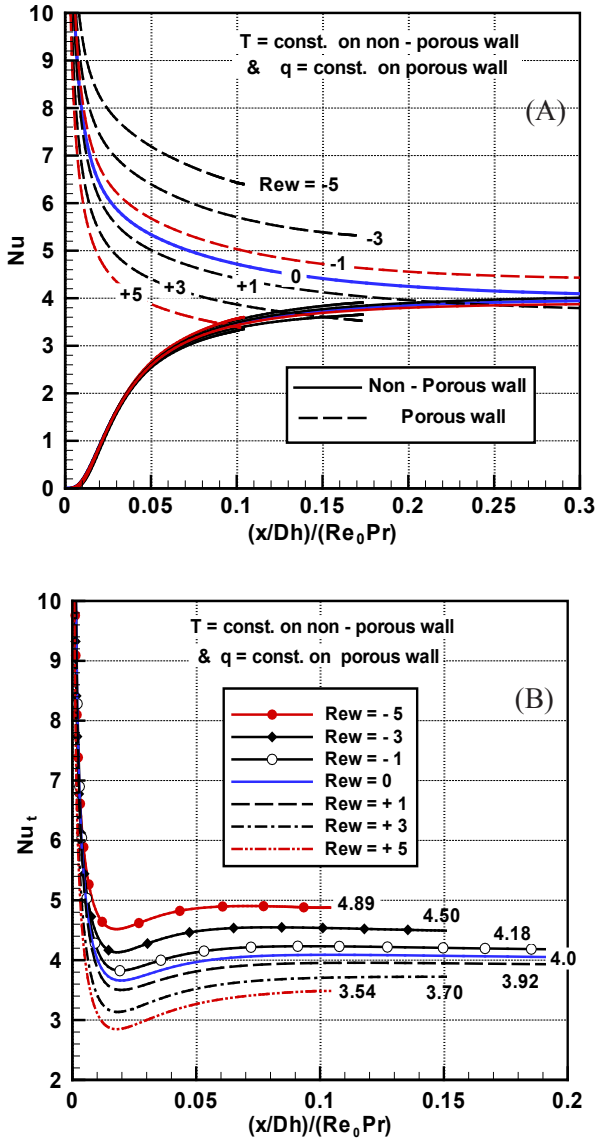

Fig. 8. Distribution of Nu number on both walls and their average Nu_t at different wall Reynolds numbers.

procedure is different than that in the previous figure. It is seen that at the porous wall the Nusselt number is larger for suction than for injection boundary condition. The opposite is true for the non-porous wall. The Nusselt number at the porous wall is equal to zero near the inlet of the channel, since similar to the previous figure temperature on the porous wall is assumed to be equal to the inlet temperature, T_0. As a result, heat transfer to the porous wall occurs only when the fluid in the channel is heated by the heat added from the porous wall. Figure 9(B) shows the distribution of

the total Nusselt number (or average value) along the channel. It is seen that beyond the entrance region near the channel inlet, the total Nusselt number for different value of Re_w becomes a constant value. Similar to the pervious figure, the Nusselt number on the porous and non-porous wall is not constant along the channel, but the total Nusselt number for the channel approaches a constant value. The total Nussel number for suction is more than that for injection and increases as the wall Reynolds number increases. The distribution of the total Nusselt number near the inlet changes when choosing a different value for wall temperature but remains the same value far from the inlet. The value of the total Nusselt number showed little change from the previous figure.

4.4. Constant and equal heat flux on Porous and non-porous walls

Figure 10 represents the variation of the local and average Nusselt number in the axial direction for a constant and equal heat flux boundary condition on both walls. In Figure 10(A) at the same wall Reynolds number, it is seen that on the porous wall heat transfer is reduced by fluid injection and is increased by fluid suction. The temperature of the porous heated wall is larger than the bulk mean temperature, therefore when injection occurs both T_w and T_m increase along the channel due to heat transfer and injected fluid along the channel. The temperature difference, $T_w - T_m$, gradually approaches a constant value in the fully developed region and the Nusselt number will be constant. In the case of suction flow, the temperature difference between the heated wall and the bulk fluid, $T_w - T_m$, is reduced due to fluid extraction, and hence the Nusselt number is larger than the injection flow at the same axial direction. Opposite results are obtained for the non–porous wall.

4.5. Constant and equal temperature on porous and non-porous walls

Figure 11 presents the distribution of the local Nusselt number along the axial direction on both walls for a

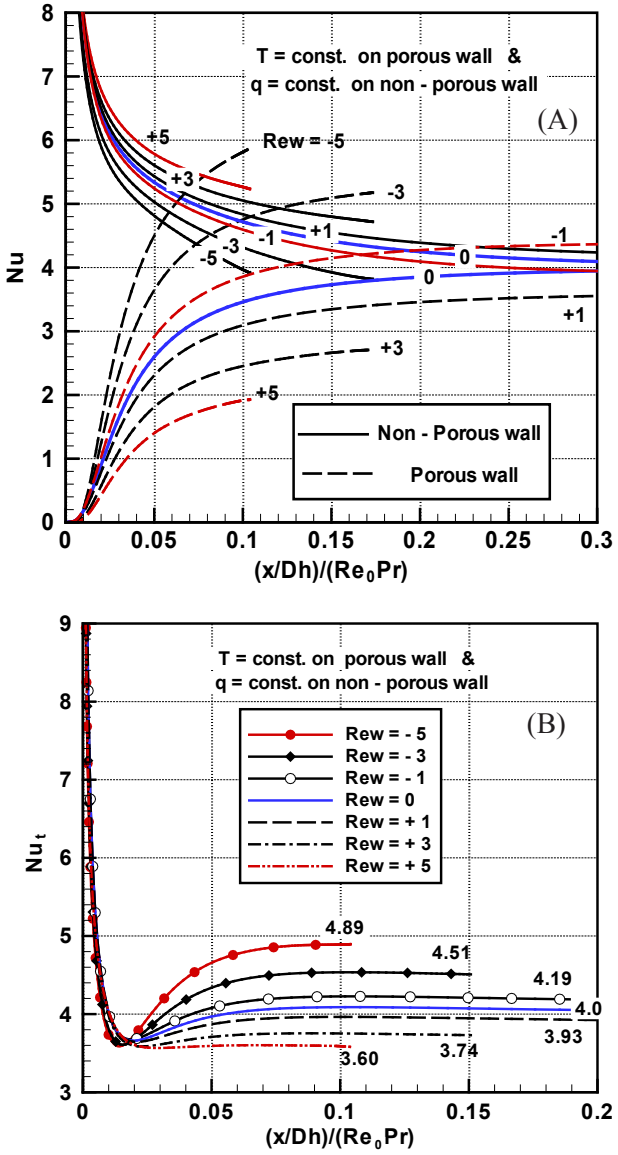

Fig. 9. Distribution of number on both walls and their average at different wall Reynolds numbers.

constant temperature boundary condition. At the same wall Reynolds number, it is seen that on the porous wall heat transfer is reduced by fluid injection and is increased by fluid suction. The temperature of the porous heated wall is larger than the bulk mean temperature for all Re_w. Wall Temperature, T_w, is constant on both walls along the channel but T_m is increased due to heat transfer and injected fluid, therefore $T_w - T_m$ will decrease along the channel. Due to heat transfer into the channel temperature gradient $-dT/dy|_{wall}$ will decrease on both walls and the Nusselt

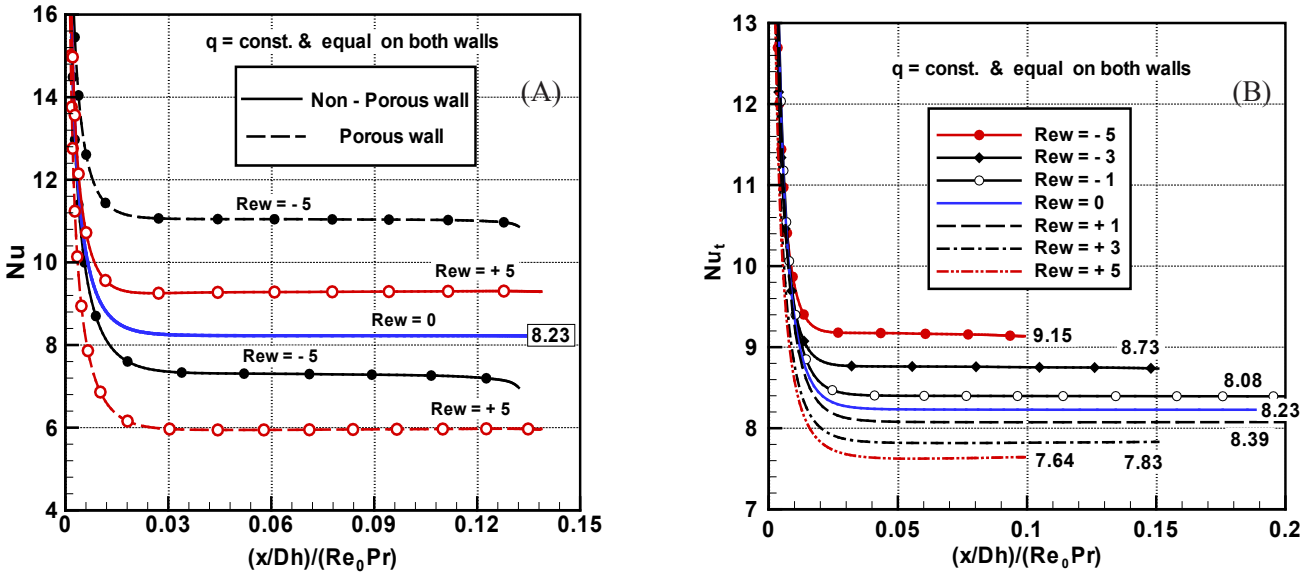

Figure 10. Distribution of number on both walls and their average at different wall Reynolds numbers

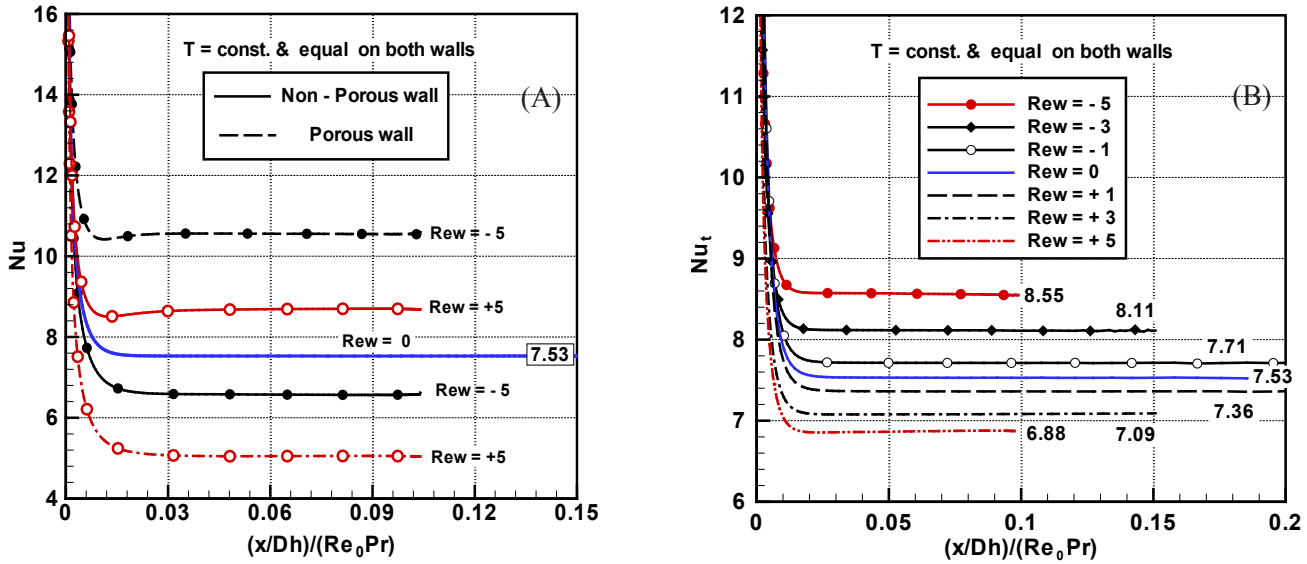

Fig.11. Distribution of number on both walls their average at different wall Reynolds numbers.

number gradually approaches a constant value in the fully developed region. In the case of suction flow the temperature difference of the heated wall and bulk fluid is reduced by fluid extraction, and hence the Nusselt number is larger than the injection flow at the same axial direction. Opposite results are obtained for the non–porous wall.

The Nusselt number is higher at the constant heat flux condition than the constant temperature condition for the same wall Reynolds number. This is similar to the normal results for these two boundary conditions for Re_w=0.

5. Conclusions

A theoretical two dimensional model was developed to simulate transport phenomena in the channel.

The channel was composed of two parallel walls, one porous and one non-porous (impermeable). To understand the behaviour of flow in this channel, the continuity, momentum and energy equations were solved when uniform air suction or injection is applied and different boundary conditions are imposed. A finite volume method was used to solve these equations. A staggered non-uniform grid system was introduced, on which the temperature and pressure were discretized and computed on the main grid, whereas velocities were computed at the staggered nodes and the equations were solved using TDMA algorithm. The results show that, at constant inlet and wall Reynolds number, the friction factor and Nusselt number on porous wall when suction occurs, are bigger than the corresponding values when injection occurs. The axial non-dimensional pressure loss in the presence of injection is larger than the corresponding values in the case of fully developed impermeable flow and also in the presence of suction. This is because the mean velocity of flow is increased along the channel in the presence of injection. In the case of suction, however, at higher suction rates the pressure tends to arrive at a constant value as the inertia and viscous forces of the flow are counterbalanced.

Nomenclature

C_f	Friction coefficient
C_p	Specific heat at constant pressure (J/kg k)
D_h	Hydraulic diameter (m)
H	Height of the channel (m)
h_H	Heat transfer coefficient (W/m^2 K)
k	Thermal conductivity
L	Length of channel (m)
Nu	Nusselt Number
P	Pressure (Pa)
Pr	Prandtl number
q	Heat flux (W/m^2)
Re	Reynolds number
Re_w	Wall Remolds number
T	Temperature (K)
u, v	Velocity components in x and y directions respectively

Greek symbols

Δ	Difference
μ	Viscosity (Pa.s)
ρ	Density
ζ	Stoichiometric ratio

Subscripts

H	Heat transfer
m	Mean value, Mass trnasfer
w	Wall
0	Inlet, Standard
t	Total

6. References

[1] A Berman, J. Applied physics , 24, 1232 , 1953.

[2] F M White, Jr., B F Baefield, and M J Goglia, J. Applied Mechanics. 25, 613,1958.

[3] J R Doughty and H C Perkins, Jr., Hydrodynamic entry length for laminar flow between parallel porous plates, Trans. ASME, J. of Applied Mechanics Vol.92, pp 548-550, 1970.

[4] J R Doughty and H C Perkins, Jr., The thermal entry problem for laminar flow between parallel porous plates, J. Heat Transfer Vol.93, pp 476-478, 1971.

[5] J R Doughty and H C Perkins, Jr., The thermal and combined entry problem for laminar flow between parallel porous plates, J. Heat Transfer Vol. 94, pp 233-234, 1972.

[6] G D Raithby and D C Knudsen, Hydrodynamic development in a duct with suction and blowing, Trans. ASME, J. Applied Mechanics, Vol.92, pp 548-550, 1970.

[7] S J Rhee and D K Edwards, Laminar entrance flow

in a flat plate duct with asymmetric suction and heating, Numerical heat transfer, Vol. 4, pp. 85-100, 1981.

[8] P Lessner and J Newman, Hydrodynamics and mass transfer in a porous-wall channel, J. Electrochem. Soc. Vol.131, pp 1828-1831, 1984.

[9] R B Kinney, Fully developed frictional and heat transfer characteristics of laminar flow in porous tubes, Int. J. Heat and mass transfer, Vol. 11, pp. 1393-1401, 1968

[10] G J Hwang and Y C Cheng, Developing laminar flow and heat transfer in square duct with one-walled injection and suction, Int. J. Heat and mass transfer, Vol. 36, pp. 2429-2440, 1993.

[11] J Yuan, M Rokni, and B Sunden, The development of heat transfer and gas flow modeling in solid oxide fuel cells, in: S. C. Singhal, M. Dokiya (Eds.), in: Solid Oxide Fuel Cells, (SOFC VI), The Electrochemical Society, Pennington, pp. 1099-1108, , 1999

[12] J Yuan, M Rokni, and B Sunden, Simulation of fully developed heat and mass transfer in fuel cell ducts with different cross-sections, International journal of heat and mass transfer, 44 (2001) 4047-4058.

[13] H Hassanzadeh, S H Mansouri, M A Mehrabian and A Sarrafi, A two-dimensional simulation of developing laminar heat and mass transfer in fuel cell channels with uniform suction of O2 and H2 " ,Proce, IMechE Vol. 222 Part A: J. Power and Energy, 2008.

[14] R K Shah and A.L. London, Laminar flow forced convection in ducts, Academic Press, New York, 1978.

[15] F P Incropera and D P Dewitt, Fundamentals of heat and mass transfer, Joun Wiley & Sons, 1990.

[16] X Li, Principles of fuel cell, Taylor & Francies, New York, 2005.

[17] H K Versteeg and W Malalasekera, An introduction to Computational Fluid Dynamics, The Finite Volume Method, Longman Scientific & Technical, England, 1995.

[18] S V Patankar, Numerical heat transfer and fluid flow, Hemisphere, Washington, DC, 1980.

[19] S Kakac, R K Shah and W Aung, Handbook of single -phase convective heat transfer, John-Wily & Sons 1987.